

ARTICLE TYPE

Voltage Control of the Boost Converter: PI vs. Nonlinear Passivity-based Control

Leyan Fang^{1,2} | Romeo Ortega² | Robert Griño³

¹Center for Control Theory and Guidance Technology, Harbin Institute of Technology, Harbin, China

²Departamento Académico de Ingeniería Eléctrica y Electrónica, ITAM, Ciudad de México, México

³Institute of Industrial and Control Engineering, Universitat Politècnica de Catalunya, Barcelona, Spain

Correspondence

Corresponding author Leyan Fang, Departamento Académico de Ingeniería Eléctrica y Electrónica, ITAM, Río Hondo 1, 01080, Ciudad de México, México.

Email: leyan.fang@itam.mx

Abstract

We carry-out a detailed analysis of *direct voltage control* of a Boost converter feeding a simple resistive load. First, we prove that using a classical PI control to stabilize a desired equilibrium leads to a very complicated dynamic behavior consisting of two equilibrium points, one of them *always unstable* for all PI gains and circuit parameter values. Interestingly, the second equilibrium point may be rendered *stable*—but for all tuning gains leading to an extremely large value of the circuit current and the controller integrator state. Moreover, if we neglect the resistive effect of the inductor, there is only one equilibrium and it is *always unstable*. From a practical point of view, it is important to note that the only useful equilibrium point is that of minimum current and that, in addition, there is always a resistive component in the inductor either by its parasitic resistance or by the resistive component of the output impedance of the previous stage. In opposition to this troublesome scenario we recall three nonlinear voltage-feedback controllers, that ensure asymptotic stability of the desired equilibrium with simple gain tuning rules, an easily defined domain of attraction and smooth transient behavior. Two of them are *very simple, nonlinear, static* voltage feedback rules, while the third one is a variation of the PID scheme called PID-Passivity-based Control (PBC). In its original formulation PID-PBC requires full state measurement, but we present a modified version that incorporates a *current observer*. All three nonlinear controllers are designed following the principles of PBC, which has had enormous success in many engineering applications.

KEYWORDS

Nonlinear control, Passivity-based control, PI control, Power converters

1 | INTRODUCTION

The ever increasing demand for smaller size, portable, and lighter weight high performance DC-DC power converters for industrial, communications, residential, and aerospace applications, has made the control of these devices a topic of widespread interest, see [15] for a recent survey. The most popular configuration for this kind of power converters is the so-called Boost converter, which provides low voltage amplification and current ratings for loads at constant switching frequency. Various attempts have been made to formulate suitable control strategies for this switching device, because its overall dynamic performance is largely determined by the controller. The task of designing a controller is complicated by the fact that the mathematical model of the Boost converter is a *bilinear* system, and its linear approximation yields very poor approximations to its behavior. An additional difficulty in the control of Boost converters is that the output signal, that is the voltage fed to the load, has the behavior of a *non-minimum phase* system [5]. Due to this behavior the vast majority of the practical controllers designed for the Boost converter are of the *indirect* type, where a PI loop is placed around the current, whose reference is determined to match the desired voltage value. This approach is clearly extremely fragile as the derivation of the current reference requires the exact knowledge of the system parameters or the design of an outer control loop for the converter output voltage, which increases the complexity of the whole controller. This issue has been extensively discussed in the literature, see *e.g.* [12, Section 4.3.A] and references therein.

In this article we analyze in detail the dynamic behavior of the classical boost converter in closed-loop with *voltage-fed* control. It is shown in the paper that there are two important factors that significantly affect the control task. First, the aforementioned non-minimum phase behavior. Second the presence (or absence) of a parasitic resistor in the input inductor. In spite of all the research carried out to study the non-minimum phase behavior of the Boost converter, to the best of our knowledge, a detailed discussion of the zero dynamics, without appealing to system linearization, has not been carried out, in particular for the case when the aforementioned resistance is taken into account.¹ As we will see in the paper the control scenario dramatically changes when this resistor is taken into account in the model.

We concentrate our attention on two types of controllers wrapped around the voltage signal. First, the well-known PI controller that, as mentioned above, is rarely used in practical applications. A detailed study of this scenario provides a definite answer on when (and when not) this configuration can be used in practice. The second type of controllers is based on the principle of *passivity*—the so-called *passivity-based controllers* (PBC) [9, 10, 16, 18]. We study two recently developed simple, static nonlinear voltage-fed PBC, and vividly illustrate their excellent dynamic performance. Finally, we also consider a variation of PID, called PID-PBC, that has attracted a lot of interest in recent years [13].

The rest of the paper has the following structure. The mathematical model of the Boost converter and some of its control properties are presented in Section 2. The first main result of the paper—that is, the analysis of the voltage-fed PI control—is given in Section 3. In Section 4 we analyze the PBCs and wrap-up the paper with some concluding remarks in Section 5. In Appendix A we present some cumbersome calculations needed to prove one of the main results.

2 | BOOST DYNAMIC MODEL AND SOME PROPERTIES

In this section we provide some background material to study the dynamic behavior of the classical boost converter in closed-loop with *voltage-fed* controllers. First, to simplify the analytic expressions we start by proposing a suitable change of coordinates and time scaling. Second, we put into evidence the property of power balance of the converter. Thirdly, we compute the assignable equilibrium set [13, Proposition B.1] and, finally, we reveal the well-known fact that the *zero dynamics* of the converter, with respect to the voltage variable, is *non-minimum phase*.

2.1 | The boost converter scaled model

Consider the (average) model of the boost converter

$$L \frac{di_L}{dt} = -Ri_L - v_c u + E \quad (1a)$$

$$C \frac{dv_c}{dt} = -Gv_c + i_L u \quad (1b)$$

where $i_L(t) \in \mathbb{R}$ is the inductor current, $v_c(t) \in \mathbb{R}$ is the capacitor voltage and $u(t) \in \mathbb{R}$ is the duty cycle. Moreover, $L > 0$ and $C > 0$ are the circuit inductance and capacitance, $R \geq 0$ is the inductor (parasitic) resistance, $G > 0$ is the load conductance and $E > 0$ is converter constant voltage source.²

Fact 1. Under the following state variable change and time scaling

$$\begin{bmatrix} x_1 \\ x_2 \end{bmatrix} = \begin{bmatrix} \frac{1}{E} \sqrt{\frac{L}{C}} & 0 \\ 0 & \frac{1}{E} \end{bmatrix} \begin{bmatrix} i_L \\ v_c \end{bmatrix}, \tau = \frac{1}{\sqrt{LC}} t,$$

¹ It should be noted that this resistive effect is due not only to the parasitic resistance in the inductor, but it appears also when we incorporate into the model the DC voltage source feeding the device—the so-called external series resistor.

² Equations (1) represent the dynamics of a bidirectional in current (and hence in power) boost converter or a unidirectional in current boost converter in its continuous conduction mode (CCM).

the system (1) admits the standard (f, g, h) representation

$$\begin{aligned}\dot{x} &= \begin{bmatrix} -d_1x_1 + 1 \\ -d_2x_2 \end{bmatrix} + \begin{bmatrix} -x_2 \\ x_1 \end{bmatrix} u \\ y &= x_2,\end{aligned}\tag{2}$$

where $\dot{x}(\tau) := \frac{dx(\tau)}{d\tau}$, $d_1 := R\sqrt{\frac{C}{L}} \geq 0$ and $d_2 := G\sqrt{\frac{L}{C}} > 0$.

Remark 1. Notice that we are considering the possibility where the resistance $R = 0$, which is a case that has often been studied. This is, however, not the case when the parasitic resistance of the inductor is considered, or the output impedance of the DC voltage source, or the previous stage, includes a resistive part.

2.2 | Power balance property

Clearly, the system (1) admits the port-Hamiltonian (pH) representation [18]

$$\dot{x} = F(u)\nabla H(x) + \begin{bmatrix} 1 \\ 0 \end{bmatrix},\tag{3}$$

with total energy function $H(x) = \frac{1}{2}|x|^2$ and the interconnection and damping matrix

$$F(u) := \begin{bmatrix} -d_1 & -u \\ u & -d_2 \end{bmatrix}.\tag{4}$$

The interest of the pH representation is that it puts in evidence the *power balance* property

$$\underbrace{\dot{H}}_{\text{stored}} = \underbrace{-d_1x_1^2 - d_2x_2^2}_{\text{dissipated}} + \underbrace{x_1 \times 1}_{\text{supplied power}},$$

which is a property satisfied by all physical systems. Notice that in the scaled model the supplied voltage E is reduced to 1—and the quantity $x_1 \times 1$ is the product of supplied voltage and extracted current. The current x_1 is the so-called “natural output” $y = g^T \nabla H$ [18].

Remark 2. One important corollary stemming from the power balance equation is that the control action, similarly to the Coriolis forces in mechanical systems, “doesn’t do any work”. Hence there are some stability properties of the system which are *independent* of the control action.

2.3 | Assignable equilibrium set

Now, applying [13, Proposition B.1], we compute the *assignable equilibrium set* and the corresponding—uniquely defined—constant control value.

Fact 2. Fix the desired equilibrium value of x_2 as $y_* > 0$. If $d_1 = 0$ there is an *unique* assignable equilibrium point given by

$$\mathcal{E}_0 = \{\bar{x} \in \mathbb{R}^2 \mid \bar{x}_1 = d_2y_*^2, \bar{x}_2 = y_*\},\tag{5}$$

with the associated constant control value

$$\bar{u} = \frac{1}{y_*}.$$

If $d_1 > 0$ the corresponding assignable equilibrium set consists of *two* points given by

$$\mathcal{E} = \{\bar{x} \in \mathbb{R}^2 \mid \bar{x}_1 = \frac{1}{2d_1} \left(1 \pm \sqrt{1 - 4d_1d_2y_*^2} \right), \bar{x}_2 = y_*\},\tag{6}$$

with the associated constant control value

$$\bar{u} = \frac{-1}{\bar{x}_1^2 + y_*^2} [(d_1 - d_2)\bar{x}_1 - 1]y_*$$

Remark 3. It is clear from (6) that, in order to ensure the existence of an equilibrium when $d_1 > 0$ it is necessary and sufficient to satisfy the constraint

$$d_1 d_2 < \frac{1}{4y_*^2}. \quad (7)$$

Notice that this constraint translates in the original coordinates into

$$RG < \frac{E^2}{4(v_c^*)^2},$$

where $v_c^* > 0$ is the desired voltage value. We bring to the readers attention the fact that we rule-out the possibility of $d_1 d_2 = \frac{1}{4y_*^2}$, which would correspond to the current been equal to $\frac{1}{2d_1}$ —which is not practically relevant.

2.4 | Zero dynamics of the boost converter with respect to the voltage

It is well-known [12, 17] that—when $d_1 = 0$ —the *zero dynamics* with respect to the output voltage of the Boost converter, is *non-minimum phase* [5]. It is, precisely, this fact that motivates most practitioners to control the converter via the so-called *indirect method*, where a PI loop is placed around the current, whose reference is determined to match the desired voltage value. This approach is clearly extremely fragile as the derivation of the current reference requires the exact knowledge of the system parameters or the design of an outer control loop for the converter output voltage, which increases the complexity of the whole controller. This issue has been extensively discussed in the literature, see *e.g.* [12, Section 4.3.A] and references therein.

In spite of all this research, to the best of our knowledge, a detailed discussion of the zero dynamics of the Boost converter, without appealing to system linearization, has not been carried out, in particular for the case when $d_1 > 0$. To alleviate this deficiency is one of the motivations of this subsection.

As is well-known, the zero-dynamics of a nonlinear system may be computed calculating its *normal form* [5] or, alternatively, computing the differential equation satisfied by the system *input*, when its output is set to a constant equilibrium value—see [12, Section 4.3.A] for the computation, via the second method, for the Boost converter. The lemma below exhibits its zero dynamics for the more general case when $d_1 > 0$. To the best of the authors' knowledge, this is the first time this result is reported.

Lemma 1. *Consider the scaled version of the dynamics of the Boost converter (2).*

F1 *Its zero dynamics, with respect to the constant output $x_2 = y_*$ is given by*

$$\dot{u} = \frac{u}{d_2} \left(u^2 - \frac{1}{y_*} u + d_1 d_2 \right). \quad (8)$$

F2 *This dynamics will have an equilibrium different from zero if and only if the condition (7) holds.*

F3 *This equilibrium is unstable.*

Proof. The differential equation (8) is obtained differentiating x_2 twice and setting $x_2 = y_*$.

Some simple calculations show that the term in parenthesis is equal to zero—that is, there is a second non-zero equilibrium—if and only if the condition (7) holds. To prove the instability of this equilibrium we study the polynomial

$$w(u) := u^2 - \frac{1}{y_*} u + d_1 d_2,$$

which has a minimum at $u_{\min} = \frac{1}{2y_*}$. It is easy to see that the non-zero equilibrium will be unstable if $w(u_{\min}) < 0$, which is the case when (7) holds. In Fig 1 we show the plot of the right hand side of (8) for two different cases.

□□□

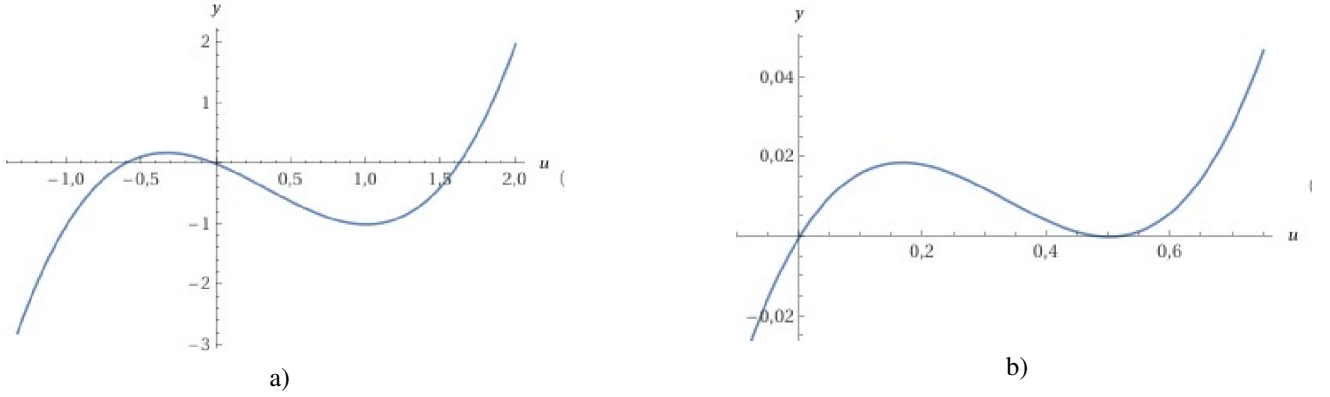


FIGURE 1 Plot of the function $y(u) = u\left(u^2 - \frac{1}{y_*}u + d_1d_2\right)$: a) Case when $d_1d_2 < \frac{1}{4y_*^2}$; b) Case when $d_1d_2 = \frac{1}{4y_*^2}$.

3 | MAIN STABILITY RESULTS FOR VOLTAGE-FED PI CONTROL

In this section we carry out the stability analysis of the PI control under the conditions of $d_1 = 0$ and $d_1 > 0$. This analysis consist of two parts, first the stability (in the Lyapunov sense) of their equilibria done invoking Lyapunov's Indirect Method [6, Theorem 4.7]. Second the determination of a domain of attraction for the case of stable equilibrium.

3.1 | PI control with $d_1 = 0$: instability of the equilibrium

In this subsection we do the (local) stability analysis of the unstable equilibrium and present some simulations that illustrate this claim.

3.1.1 | Instability of the equilibrium

Proposition 1. Consider the system (2) with $d_1 = 0$ in closed-loop with the PI control

$$\begin{aligned} \dot{x}_c &= y_* - x_2 \\ u &= u_0 + K_I x_c + K_P (y_* - x_2), \end{aligned} \quad (9)$$

with the PI gains $K_P \geq 0$, $K_I > 0$ and $u_0 \in \mathbb{R}$ a designer chosen parameter. The closed-loop system has a unique equilibrium point which is unstable for all settings of the tuning gains.

Proof. Define the state variables $\chi := \text{col}(x_1, x_2, x_c)$. The system (2) with $d_1 = 0$ in closed-loop with the PI controller (9) is of the form

$$\dot{\chi} = \begin{bmatrix} 1 - u_0\chi_2 - K_I\chi_2\chi_3 - K_P\chi_2y_* + K_P\chi_2^2 \\ -d_2\chi_2 + u_0\chi_1 + K_I\chi_1\chi_3 + K_P\chi_1y_* - K_P\chi_1\chi_2 \\ -\chi_2 + y_* \end{bmatrix} =: f(\chi). \quad (10)$$

Invoking Lyapunov's Indirect Method [6, Theorem 4.7], we will prove the instability claim of Proposition 1. Towards this end, we compute the Jacobian of the vector field $f(\chi)$ as

$$\nabla f(\chi) = \begin{bmatrix} 0 & -u_0 - K_I\chi_3 - K_Py_* + 2K_P\chi_2 & -K_I\chi_2 \\ u_0 + K_I\chi_3 + K_Py_* - K_P\chi_2 & -d_2 - K_P\chi_1 & K_I\chi_1 \\ 0 & -1 & 0 \end{bmatrix}.$$

Evaluating the Jacobian at the equilibrium $\bar{\chi} = \text{col}(\bar{\chi}_1, y_*, \bar{\chi}_3)$ yields

$$\nabla f(\bar{\chi}) = \begin{bmatrix} 0 & -u_0 - K_I\bar{\chi}_3 + K_Py_* & -K_Iy_* \\ u_0 + K_I\bar{\chi}_3 & -d_2 - K_P\bar{\chi}_1 & K_I\bar{\chi}_1 \\ 0 & -1 & 0 \end{bmatrix}.$$

The characteristic polynomial of this matrix is of the form $p(\lambda) := \lambda^3 + a_2\lambda^2 + a_1\lambda + a_0$, with

$$\begin{aligned} a_0 &:= -K_I(K_I\bar{\chi}_3 + u_0)y_* \\ a_1 &:= K_I^2\bar{\chi}_3^2 + (2u_0\bar{\chi}_3 + \bar{\chi}_1 - K_P\bar{\chi}_3y_*)K_I - u_0y_*K_P + u_0^2 \\ a_2 &:= K_P\bar{\chi}_1 + d_2. \end{aligned}$$

Based on the Routh-Hurwitz criterion, all roots of the characteristic polynomial will have negative real parts (i.e., system is stable) if and only if

$$a_0 > 0, \quad a_1 > 0, \quad a_2 > 0, \quad a_2a_1 > a_0. \quad (11)$$

We now evaluate the equilibrium $\bar{\chi}_3$ as

$$\bar{\chi}_3 = \frac{1}{K_I y_*} (1 - u_0 y_*),$$

which upon replacement in a_0 yields $a_0 = -K_I < 0$ —violating the first condition of (11). Hence, the equilibrium is *unstable* for all circuit parameters and settings of the PI gains. $\square\square\square$

Remark 4. This result proves that the claim of Proposition 3 (and consequently also the main result of Theorem 2) in [1] is wrong.

Remark 5. Notice that, setting $K_P = 0$, we also prove that the pure integral control is also unstable for all values of $K_I > 0$.

3.1.2 | Simulation results

In Fig. 2 we present simulations of the closed-loop system (10) with different initial conditions for the following parameters:

$$y_* = 2, \quad d_2 = 1, \quad K_I = 1, \quad K_P = 2, \quad u_0 = \frac{1}{2}.$$

From the figure it is clear that the equilibrium χ^u is, indeed, unstable.

It was observed that the surface

$$\mathcal{S}_0 := \{(\chi_1, \chi_2) \mid \chi_1 - d_2\chi_2^2 = 0\},$$

which clearly contains the assignable equilibrium point given in (5), defines a separatrix, in the sense that taking initial conditions “below” the surface yields trajectories for $(\chi_1(t), \chi_2(t))$ converging to $(0, 0)$. On the other hand, with initial conditions “above” the surface the trajectory of $\chi_1(t)$ diverges to infinity. It is interesting to note that this surface precisely coincides with the place where the derivative of the systems energy $H(x)$ equal zero. Indeed, from (3) it is easy to see that, when $d_1 = 0$, we have

$$\dot{H} = -d_2x_2^2 + x_1.$$

This is consistent with the fact that “below” the surface $\dot{H} < 0$ and the energy decreases to zero. Unfortunately, no further analysis of this interesting behavior has been carried out.

3.2 | PI control with $d_1 > 0$: stability/instability of the equilibria

In this subsection we do the (local) stability analysis of equilibrium when $d_1 > 0$ and present some simulations that illustrate the claims.

3.2.1 | Stability/Instability of the equilibrium

Proposition 2. Consider the system (2) with $d_1 > 0$, verifying the equilibrium existence condition (7), in closed-loop with the PI control (9).

C1 The closed-loop system has two equilibrium points, consistent with $\bar{\chi}_2 = y_*$, denoted

$$\begin{aligned} \bar{\chi}^u &:= (\bar{\chi}_1^u, y_*, \bar{\chi}_3^u) \in \mathbb{R}^3 \\ \bar{\chi}^s &:= (\bar{\chi}_1^s, y_*, \bar{\chi}_3^s) \in \mathbb{R}^3, \end{aligned}$$

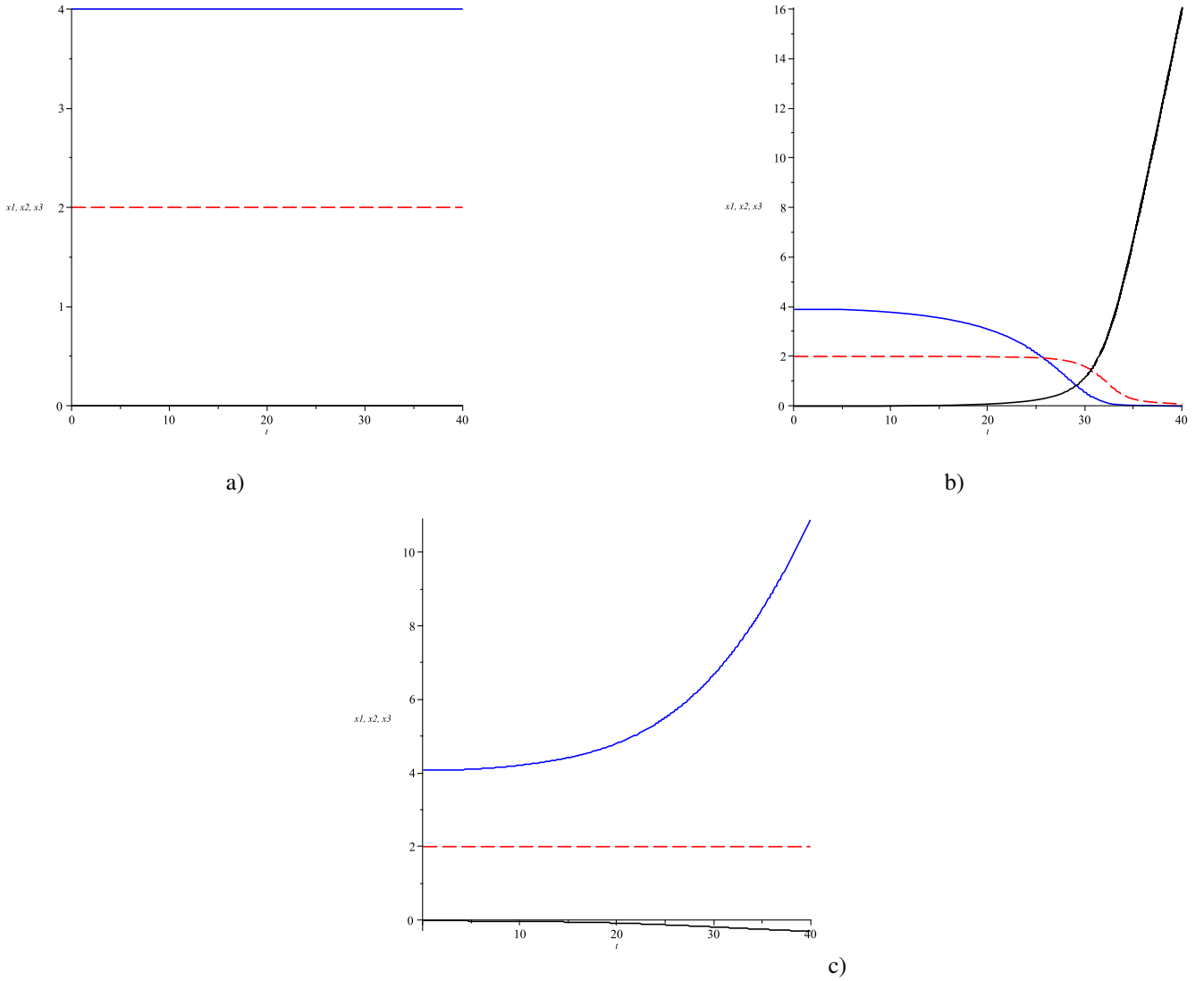


FIGURE 2 Transient behavior of the closed-loop system (10) with different initial conditions: a) at the unstable equilibrium point $\chi^u(0) = (4, 2, 0)$; b) at $\chi^u(0) = (3.9, 2, 0)$; c) at $\chi^u(0) = (4.1, 2, 0)$. χ_1 –blue, χ_2 –dotted red and χ_3 –black.

whose explicit expressions are given in (14) in the the proof below.

C2 $\bar{\chi}^u$ is unstable for all choices of the tuning gains.

C3 $\bar{\chi}^s$ is asymptotically stable provided the following inequalities hold:³

$$K_P \geq \frac{1}{2} d_1^2, \quad (12a)$$

$$K_I \geq \frac{5}{16} \frac{d_1}{y_*^2}. \quad (12b)$$

C4 A domain of attraction associated to $\bar{\chi}^s$ is given by

$$\mathcal{D} := \{\chi \in \mathbb{R}^3 \mid \chi^\top P \chi \leq \rho_{\mathcal{D}}, \rho_{\mathcal{D}} > 0\},$$

³ As seen in the proof there are many other options of the various gains that will ensure asymptotic stability. The one given in (12) is just one particular example, which is easy to satisfy because d_1 is, in general, a small number.

with $P \in \mathbb{R}^{n \times n}$ a positive definite matrix satisfying the algebraic Lyapunov equation (19) for any positive definite matrix $Q \in \mathbb{R}^{2 \times 2}$ and $\rho_{\mathcal{D}}$ is a sufficiently small constant.

Proof. The closed-loop dynamics takes the form

$$\dot{\chi} = \begin{bmatrix} -d_1\chi_1 + 1 - u_0\chi_2 - K_I\chi_2\chi_3 - K_P\chi_2y_* + K_P\chi_2^2 \\ -d_2\chi_2 + u_0\chi_1 + K_I\chi_1\chi_3 + K_P\chi_1y_* - K_P\chi_1\chi_2 \\ -\chi_2 + y_* \end{bmatrix} =: f(\chi). \quad (13)$$

Claim **C1** follows from the definition of the assignable equilibrium set (6) leading to

$$\bar{\chi}^u := \begin{bmatrix} \frac{1}{2d_1} \left(1 - \sqrt{1 - 4d_1d_2y_*^2} \right) \\ y_* \\ \frac{1}{K_I y_*} \left(1 - d_1\bar{\chi}_1^u - u_0y_* \right) \end{bmatrix}, \quad \bar{\chi}^s := \begin{bmatrix} \frac{1}{2d_1} \left(1 + \sqrt{1 - 4d_1d_2y_*^2} \right) \\ y_* \\ \frac{1}{K_I y_*} \left(1 - d_1\bar{\chi}_1^s - u_0y_* \right) \end{bmatrix}, \quad (14)$$

with the associated constant control values

$$\bar{u}^u := \frac{-1}{(\bar{\chi}_1^u)^2 + y_*^2} [(d_1 - d_2)\bar{\chi}_1^u - 1]y_*$$

$$\bar{u}^s := \frac{-1}{(\bar{\chi}_1^s)^2 + y_*^2} [(d_1 - d_2)\bar{\chi}_1^s - 1]y_*.$$

Invoking Lyapunov's Indirect Method [6, Theorem 4.7], we will prove the claims **C2** and **C3** of Proposition 2. Towards this end, we compute the Jacobian of the vector field $f(\chi)$ as

$$\nabla f(\chi) = \begin{bmatrix} -d_1 & -u_0 - K_I\chi_3 - K_P y_* + 2K_P\chi_2 & -K_I\chi_2 \\ u_0 + K_I\chi_3 + K_P y_* - K_P\chi_2 & -d_2 - K_P\chi_1 & K_I\chi_1 \\ 0 & -1 & 0 \end{bmatrix}.$$

Evaluating the Jacobian at the equilibrium $\bar{\chi} = \text{col}(\bar{\chi}_1, y_*, \bar{\chi}_3)$ yields

$$\nabla f(\bar{\chi}) = \begin{bmatrix} -d_1 & -u_0 - K_I\bar{\chi}_3 + K_P y_* & -K_I y_* \\ u_0 + K_I\bar{\chi}_3 & -d_2 - K_P\bar{\chi}_1 & K_I\bar{\chi}_1 \\ 0 & -1 & 0 \end{bmatrix}.$$

The characteristic polynomial of this matrix is of the form $p(\lambda) := \lambda^3 + a_2\lambda^2 + a_1\lambda + a_0$, with

$$a_0 := -K_I(K_I\bar{\chi}_3y_* - d_1\bar{\chi}_1 + u_0y_*)$$

$$a_1 := K_I^2\bar{\chi}_3^2 + (2u_0\bar{\chi}_3 + \bar{\chi}_1 - K_P\bar{\chi}_3y_*)K_I + (d_1\bar{\chi}_1 - u_0y_*)K_P + d_1d_2 + u_0^2$$

$$a_2 := K_P\bar{\chi}_1 + d_1 + d_2.$$

As indicated in the proof of Proposition 1, the inequalities (11) are the necessary and sufficient condition for (local) stability of the equilibria. In the sequel we will verify these conditions for the two different equilibrium points of the closed-loop system.

Case of minimal current The minimal current equilibrium is associated with the unstable equilibrium and is given as

$$\bar{\chi}_1^u := \frac{1}{d_1} \left(\frac{1}{2} - r \right), \quad (15)$$

where for ease of future reference we have defined the constant

$$r := \frac{1}{2} \sqrt{1 - 4d_1d_2y_*^2} > 0.$$

The corresponding equilibrium for $\bar{\chi}_3^u$ is then

$$\bar{\chi}_3^u = \frac{1}{K_I y_*} \left(\frac{1}{2} + r - u_0y_* \right). \quad (16)$$

After some algebraic operations we can evaluate a_0 with (15) and (16) getting

$$a_0 = -2K_I r,$$

which is always negative, proving claim **C2**.

Case of maximal current We repeat here the same steps above for the maximal current equilibrium. The maximal current equilibrium and its associated component for $\bar{\chi}_3^s$ are given as⁴

$$\begin{aligned}\bar{\chi}_1^s &:= \frac{1}{d_1} \left(\frac{1}{2} + r \right) \\ \bar{\chi}_3^s &= \frac{1}{K_I y_*} \left(\frac{1}{2} - r - u_0 y_* \right).\end{aligned}\tag{17}$$

Some lengthy, but straightforward calculations with these two equations yields

$$\begin{aligned}a_0 &= 2K_I r \\ a_1 &= \frac{1}{4d_1 y_*^2} \left(4d_1^2 d_2 y_*^2 + 8r K_P y_*^2 d_1 + 4 \left(r - \frac{1}{2} \right)^2 d_1 + 4K_I y_*^2 \left(\frac{1}{2} + r \right) \right) \\ a_2 &= \frac{K_P}{d_1} \left(\frac{1}{2} + r \right) + d_1 + d_2.\end{aligned}$$

which are all positive. It remains only to prove that

$$a_1 a_2 - a_0 > 0.\tag{18}$$

In Appendix A we present the Maple calculations that compute (18) multiplied by a positive factor, denoted f_1 . From these expressions we identify three polynomials that recover all the negative terms appearing in f_1 , namely:

$$\begin{aligned}p_1(r) &:= d_1^3 (8r^2 - 8r + 2) \\ p_2(r) &:= d_2 d_1^2 (8r^2 - 8r + 2) + d_1^2 (-8K_I y_*^2 r + 4K_I y_*^2) \\ p_3(r) &:= 8K_P d_1 r \left(r^2 - \frac{1}{2}r - \frac{1}{4} \right)\end{aligned}$$

Applying to these polynomials the following equivalence

$$p(r) := r^2 + ar + b \geq 0 \iff 4b \geq a^2,$$

we conclude that $p_1(r)$ is always nonnegative. Regarding $p_2(r)$, note that its first term on the right-hand side is clearly nonnegative, and its second term is larger equal to $-4K_I y_*^2 d_1^2 r^2$, which yields

$$\begin{aligned}p_2(r) &\geq d_2 d_1^2 (8r^2 - 8r + 2) + 4K_I y_*^2 d_1^2 (r - 1)^2 - 4K_I y_*^2 d_1^2 r^2 \\ &\geq -4K_I y_*^2 d_1^2 r^2.\end{aligned}$$

To dominate this term we take the term $8K_P K_I y_*^2 r^2$, which appears in the last right hand side product of f_1 , thus ensuring the inequality (12a) holds.

Regarding $p_3(r)$ it is easy to show that the second order polynomial is larger equal to $-\frac{5}{16}$, hence we have

$$p_3(r) \geq -\frac{5}{2} K_P d_1 r.$$

To dominate this term we take the term $8K_P K_I y_*^2 r$, which appears in the last right hand side product of f_1 , provided that the inequality (12b) holds. Hence, the claim **C3** is proved.

To prove the claim **C4** we define the Lyapunov equation

$$A^\top P + PA = -Q,\tag{19}$$

⁴ Notice that the minimal and maximal current equilibria differ only on the sign of the constant r .

where we defined the matrix

$$A := \nabla f(\chi^3),$$

and recall that the positive definite function $V(\delta\chi) := \delta\chi^\top P\delta\chi$ qualifies as a Lypunov function for the linearized system

$$\dot{\delta\chi} = A\delta\chi.$$

□□□

3.2.2 | Simulation results

In Figs. 3 and 4 we present simulations of the closed-loop system (13) with different initial conditions for the following parameters:

$$y_* = 1, d_1 = \frac{1}{4}, d_2 = \frac{3}{4}, K_I = 1, K_P = 2, u_0 = \frac{1}{2}.$$

First, we set the initial conditions at (and close) the unstable equilibrium $\bar{\chi}^u$ associated to the minimum current. Then, we tune the gains to ensure the equilibrium associated to the maximal current is stable verifying (18) and, again, set the initial conditions at (and close) the stable equilibrium $\bar{\chi}^s$.

As shown in Figs. 3 and 4, the instability of χ^u and the stability of χ^s are evident, thereby corroborating Proposition 2.

Similarly to the case $d_1 = 0$, the surface

$$\mathcal{S}_u := \{(\chi_1, \chi_2) \mid \chi_1 - d_1\chi_1^2 - d_2\chi_2^2 = 0\},$$

which clearly contains the assignable equilibrium point given in (6), defines a separatrix with the same properties as \mathcal{S}_0 . Again, this surface precisely coincides with the place where the derivative of the systems energy $H(x)$ equal zero.

4 | VOLTAGE FEEDBACK PASSIVITY-BASED CONTROL

In this section we recall three voltage feedback controllers which ensure global regulation of the voltage signal. All three of them are designed following the approach of PBC [9], which has had enormous success in applications. The first two schemes are nonlinear voltage-feedback static controllers, and have been reported in [14] and [19], respectively. They both belong to the class of Interconnection and Damping Assignment (IDA)-PBC first reported in [10, 11]. The third one is a PID-PBC, first reported in [4] and further developed in [2, 13].

4.1 | Two nonlinear output feedback controllers

We give below, without proof, the propositions pertaining to the two static controllers reported in [14] and [19], respectively. The proofs may be found in the corresponding reference.

Proposition 3. [14] Consider the Boost converter model (2) with $d_1 = 0$ in closed-loop with the IDA-PBC

$$u = \frac{1}{y_*} \left(\frac{x_2}{y_*} \right)^\alpha, \quad (20)$$

where $\alpha \in (0, 1)$ is a tuning gain. Then, the equilibrium point $x_* := (d_2 y_*^2, y_*)$ is asymptotically stable.

Proposition 4. [19] Consider the Boost converter model (2) with $d_1 = 0$ in closed-loop with the IDA-PBC

$$u = k \frac{x_2}{x_2^2 + (k-1)y_*^2}, \quad (21)$$

where $k > 3$ is a tuning gain.

P1 The equilibrium point $x_* := (d_2 y_*^2, y_*)$ is asymptotically stable.

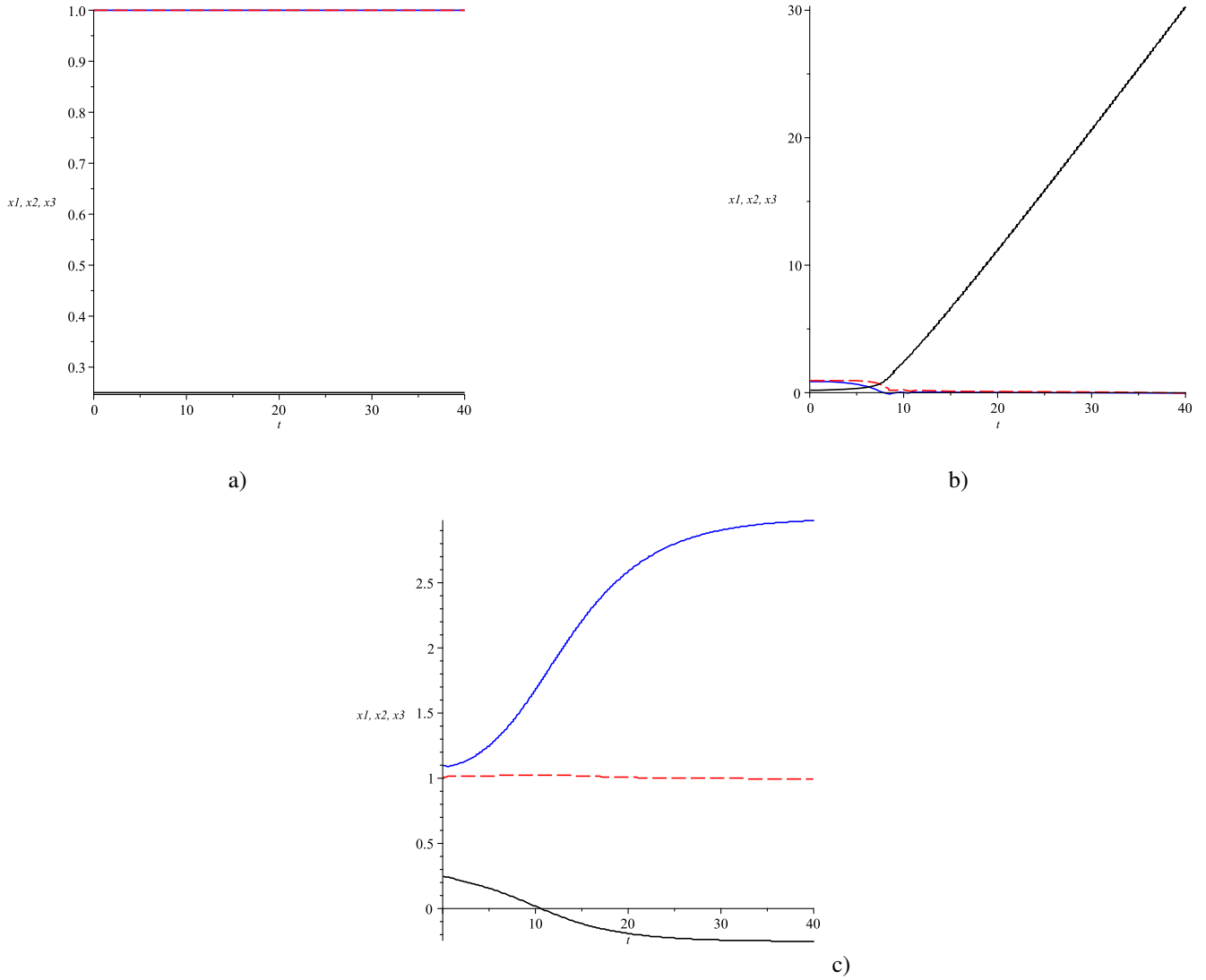


FIGURE 3 Transient behavior of the closed-loop system (13) with different initial conditions: a) at the unstable equilibrium point $\chi^u(0) = (1, 1, \frac{1}{4})$; b) at $\chi^u(0) = (0.9, 1, \frac{1}{4})$; c) at $\chi^u(0) = (1.1, 1, \frac{1}{4})$. χ_1 –blue, χ_2 –dotted red and χ_3 –black.

P2 *There exists a domain of attraction, defined by a Lyapunov function⁵, that guarantees that if we start in this set, the state $x(t)$ remains in the positive quadrant.*

Simulation results

In Figs. 5 and 6 below we show some simulation results of the two controllers above. As seen in the figures both controllers ensure asymptotic stability of the desired equilibrium. Some other properties, pertaining to the performance of the controllers, *e.g.*, domain of attraction, speed of convergence, etc, may be found in [14] and [19].

Remark 6. The simplicity of both controllers can hardly be overestimated. Consisting only of some very simple algebraic operations. Also, it should be underscored that the neither one of the controllers require *any prior knowledge* about the converter parameters, making them robust with respect to parameter uncertainty.

⁵ The expression of $P(x)$ is given in [19] of the closed-loop dynamics $P(x)$

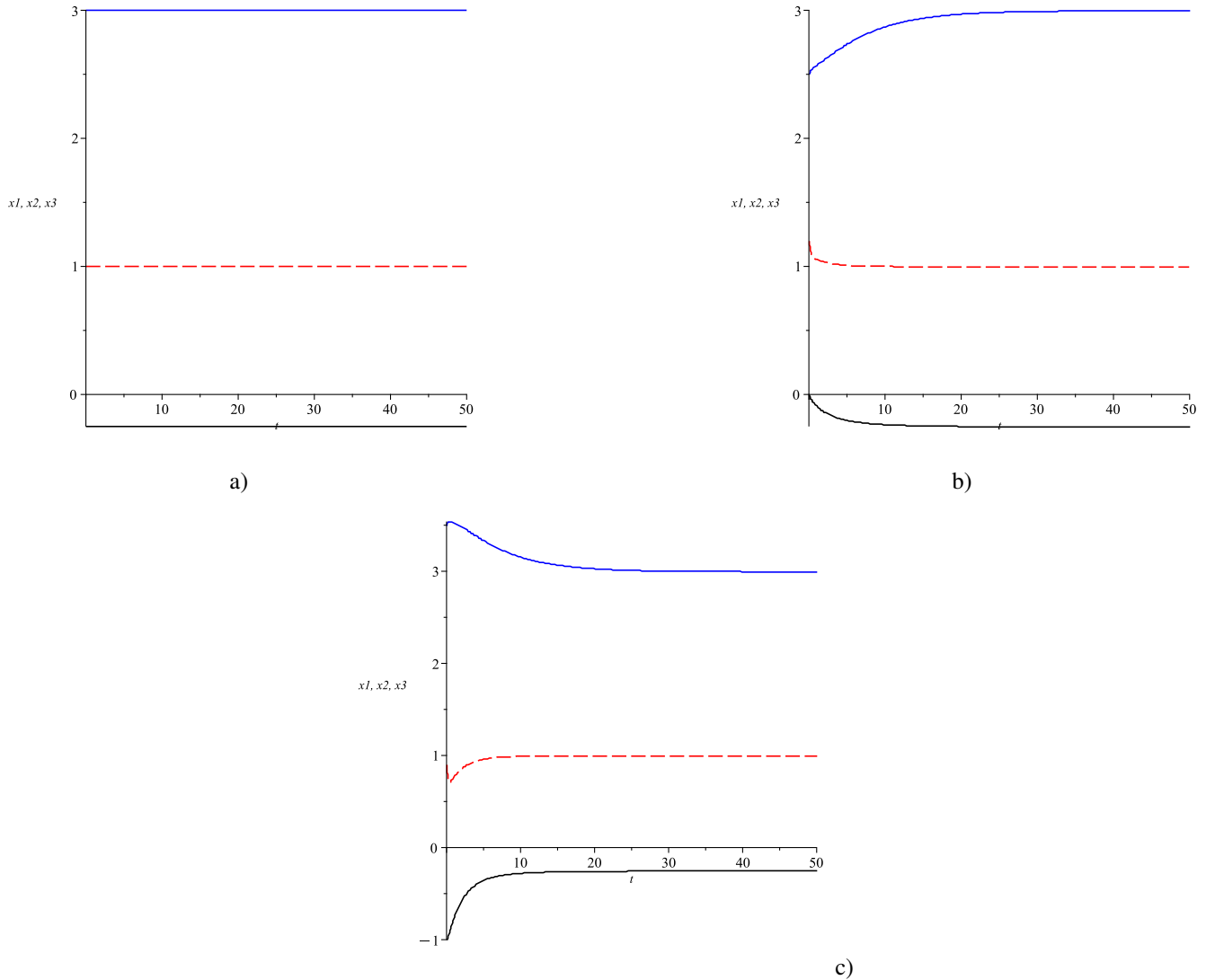


FIGURE 4 Transient behavior of the closed-loop system (13) verifying (18) with different initial conditions: a) at the stable equilibrium point $\chi^s(0) = (3, 1, -\frac{1}{4})$; b) at $\chi^s(0) = (2.5, 1.2, 0)$; c) at $\chi^s(0) = (3.5, 0.9, -1)$. χ_1 —blue, χ_2 —dotted red and χ_3 —black.

Remark 7. One drawback of the two propositions above is that it is assumed that the parasitic resistance d_1 is equal to zero. Current research is under way to extend these results for the case $d_1 \neq 0$.

4.2 | A PID passivity-based controller

We finish this section presenting the PID-PBC reported in [2]. This scheme is an output-feedback version of the original PID-PBC first reported in [4] and further developed in [13]. The main contribution of [2] is that, implementing an adaptive observer, removed the need for the *full state* feedback required in [4]. Another interesting feature of the PID-PBC is that it is applicable to a large class of power converters, in contrast to the schemes in [14] and [19], which are developed for the Boost converter only—moreover, for the Boost converter the PID-PBC design does not need to assume $d_1 = 0$. The prize that is paid for these generalizations is in the *complexity* of the implementation that, as will be seen below, is several orders of magnitude bigger than the two static controllers of Propositions 3 and 4.

As explained above, the controller in [2] consists of a state observer and a PID-PBC of the form given in [4, 13]. To simplify the presentation we split the main stability result in two parts: first, the design of the state observer for the Boost converter model

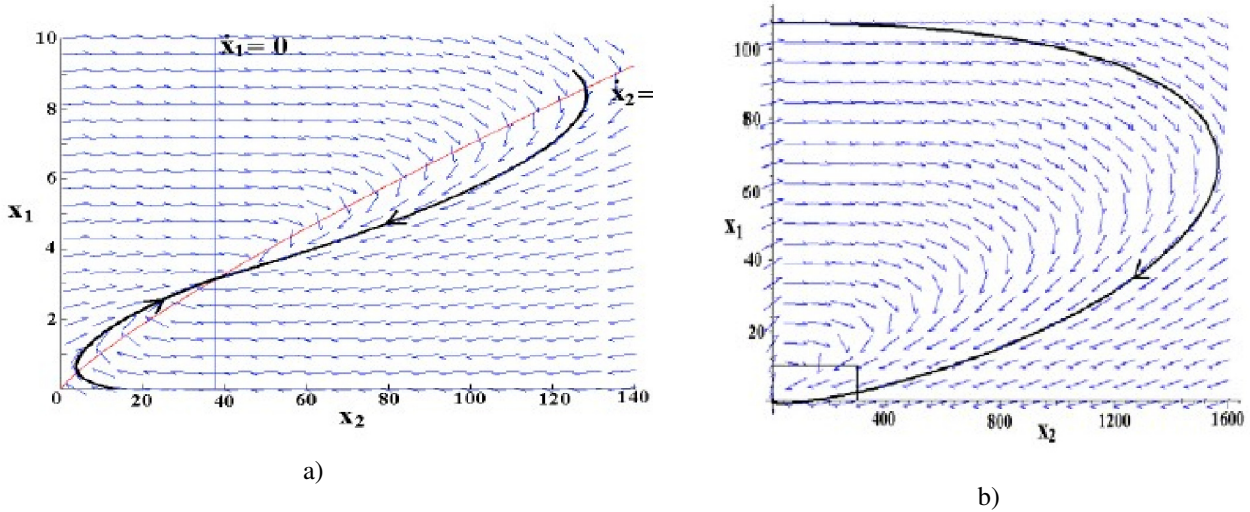


FIGURE 5 a) Phase plane of the converter model in closed-loop with the control (20), showing one trajectory (in black); b) an enlarged view illustrating the large size of the domain of attraction (see the scales).

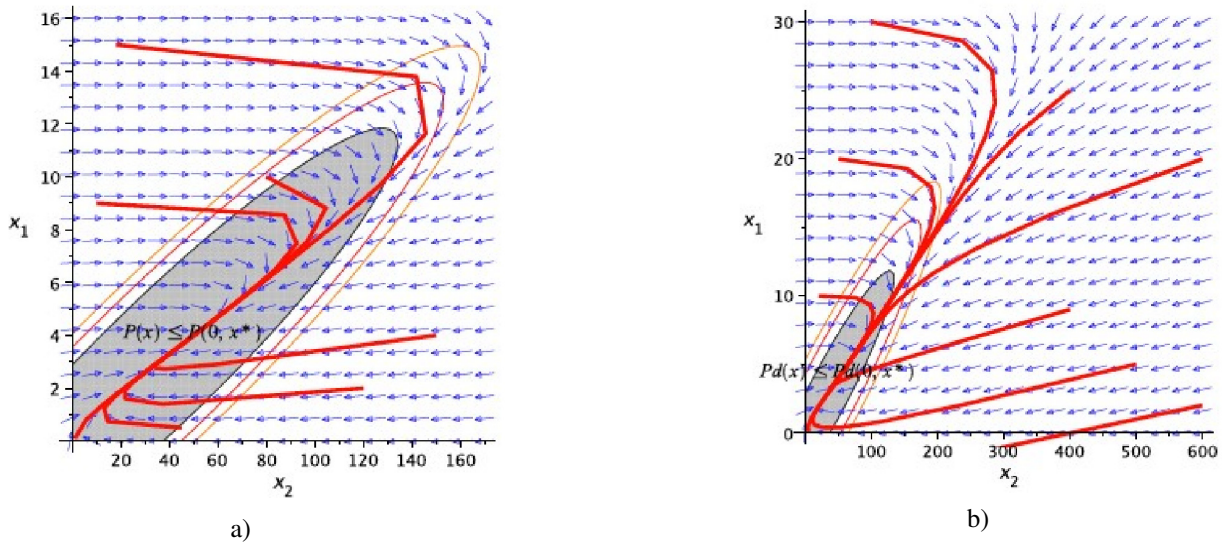


FIGURE 6 a) Phase plane of the converter model in closed-loop with the control (21), showing some trajectories (in red) and an estimate of the domain of attraction that—as indicated by the arrows—ensures $x(t) > 0$ (in gray); b) An enlarged version.

(2). Second, the implementation of a *certainty equivalent* version of the PID-PBC of [4, 13], where the actual converter current is replaced by its estimate generated by the observer. It should be underscored that the observer has *finite convergence time* (FCT) properties, hence the good behavior of the certainty equivalent PID-PBC is guaranteed.

In the proposition below we propose a state observer that ensures FCT of the estimated state, under the following extremely weak interval excitation assumption [7] on a scalar signal Δ , which is defined below.

Assumption 1. Fix a small constant $\mu \in (0, 1)$ and a positive number γ . There is a time $t_c \in (0, \infty)$ such that

$$\int_0^{t_c} \Delta^2(\tau) d\tau \geq -\frac{1}{\gamma} \ln(1 - \mu). \quad (22)$$

Proposition 5. [2] Consider the Boost converter model (3) with measurable output the voltage

$$y = Cx = [0 \ 1]x = x_2.$$

Define the observer via

$$\dot{\xi} = F(u)\xi + \begin{bmatrix} 1 \\ 0 \end{bmatrix} \quad (23a)$$

$$\dot{\Phi} = F(u)\Phi, \quad \Phi(0) = I_2 \quad (23b)$$

$$\dot{Y} = -\lambda Y + \lambda \Phi^\top C^\top (C\xi - y) \quad (23c)$$

$$\dot{\Omega} = -\lambda \Omega + \lambda \Phi^\top C^\top C \Phi \quad (23d)$$

$$\dot{\omega} = -\gamma \Delta^2 \omega, \quad \omega(0) = 1 \quad (23e)$$

$$\dot{\hat{\theta}} = \gamma \Delta (\mathcal{Y} - \Delta \hat{\theta}), \quad (23f)$$

with $F(u)$ given in (4), $\lambda > 0$, $\gamma > 0$, free tuning parameters and

$$\mathcal{Y} := \text{adj}\{\Omega\}Y, \quad \Delta := \det\{\Omega\}, \quad (24)$$

where $\text{adj}\{\cdot\}$ is the adjunct matrix. The state estimate

$$\hat{x} = \xi + \Phi \hat{\theta}_{\text{FCT}} \quad (25)$$

where we introduced the vector

$$\hat{\theta}_{\text{FCT}} := \frac{1}{1 - \omega_c} \left[\hat{\theta} - \omega_c \hat{\theta}(0) \right], \quad (26)$$

and ω_c is defined via the clipping function

$$\omega_c = \begin{cases} \omega & \text{if } \omega \leq 1 - \mu, \\ 1 - \mu & \text{if } \omega > 1 - \mu. \end{cases}$$

ensures that, for all initial conditions $(x(0), \xi(0), Y(0), \Omega(0), \hat{\theta}(0)) \in \mathbb{R}^2 \times \mathbb{R}^2 \times \mathbb{R}^2 \times \mathbb{R}^{2 \times 2} \times \mathbb{R}^2$, we have that

$$\hat{x}(t) = x(t), \quad \forall t > t_c \quad (27)$$

with all signals bounded provided Δ verifies Assumption 1.

As thoroughly discussed in [4, 13] the key step in the implementation of the PI-PBC is the generation of an output signal that is *shifted passive* [13, Section 4.2.1]. This property combined with the well-known passivity of the PI ensures stability of the closed-loop. Equipped with the FCT state observer of Proposition 5 we can implement a (certainty equivalent) voltage-feedback PID-PBC as follows.

Proposition 6. [2] Consider the Boost converter model (3) in closed-loop with the PID-PBC

$$\begin{aligned} \dot{x}_c &= y_{PI} \\ u &= -K_P y_{PI} - K_I x_c, \end{aligned} \quad (28)$$

where

$$y_{PI} = x_1^* x_2 - y_* \hat{x}_1,$$

with $\hat{x}_1(t) \in \mathbb{R}$ the estimate of x_1 generated in Proposition 5. Then, the equilibrium point $(\bar{x}_1, \bar{x}_2, \bar{x}_c) := (d_2 y_*^2, y_*, 0)$ is asymptotically stable.

5 | CONCLUDING REMARKS AND FUTURE RESEARCH

We have carried out a detailed analysis of the behavior of the Boost converter under the action of *voltage output* controllers. We have considered the classical PI control and three different classes of PBC. We have proven the important role of the inductor parasitic resistance (R in (1)) showing, in particular, that the PI controller is *always* unstable if $R = 0$. In the alternative case that $R > 0$ we proved that the dynamics of the PI control exhibits two equilibria, one of them *always* unstable and the other one stable for *sufficiently large* PI gains. But it is important to note that the equilibrium of practical interest (the one with the lowest inductor current) corresponds to the unstable case.

Regarding the PBC controllers, we presented two very simple nonlinear static voltage feedback controllers, exhibiting *excellent* dynamic performance. Both schemes are restricted to the particular case when $R = 0$. Current research is under way to extend the results of the PBC to consider $R > 0$. Two additional research lines we are pursuing for the PBCs are, on one hand, to extend their application to other DC-to-DC converter topologies, *e.g.*, Buck-Boost or Ćuk and to consider other type of loads, for instance, *constant power loads or a combination of resistive and constant power loads*. Finally, we expect to be able to carry out experimental work of the proposed controller topologies in the near future.

References

1. J. Alvarez and G. Espinosa, Stability of current-mode control for DC-DC power converters, *Systems and Control Letters*, vol. 45, pp. 113-119, 2002.
2. A. Bobtsov, R. Ortega, N. Nikolayev and W. He, A globally stable practically implementable PI passivity-based controller for switched power converters, *Int. J. on Adaptive Control and Signal Processing*, vol. 35, no. 11, pp. 2155-2174, 2021.
3. M. Fliess, Generalized controller canonical forms for linear and nonlinear dynamics, *IEEE Trans. Automatic Control*, vol. 35, pp. 994-1001, 1990.
4. M. Hernandez-Gomez, R. Ortega, F. Lamnabhi-Lagarrigue and G. Escobar, Adaptive PI stabilization of switched power converters, *IEEE Trans. Control Systems Technology*, vol. 18, no. 3, pp. 688-698, 2008.
5. A. Isidori, *Nonlinear Control Systems*, Springer-Verlag, 1995.
6. H. Khalil, *Nonlinear Systems*, Third Ed., Pearson, 2005.
7. G. Kreisselmeier and G. Rietze-Augst, Richness and excitation on an interval—with application to continuous-time adaptive control, *IEEE Transactions on Automatic Control*, vol. 35, no. 2, pp. 165-171, 1990.
8. R. D. Middlebrook and S. Ćuk, A general unified approach to modelling switching-sonverter power stages, *PESC*, pp. 18-34, 1976.
9. R. Ortega, A. van der Schaft. I. Mareels and B. Maschke B, Putting energy back in control, *IEEE Control Systems Magazine*, vol 21, no. 2, pp. 18-33, 2001.
10. R. Ortega, A. van der Schaft, B. Maschke and G. Escobar, Interconnection and damping assignment passivity-based control of port-controlled Hamiltonian systems, *Automatica*, vol. 38, no. 4, pp. 585-596, April 2002.
11. R. Ortega and E. Garcia-Canseco, Interconnection and damping assignment passivity-based control: A survey, *European J. of Control*, vol. 10, pp. 432-450, 2004.
12. R. Ortega, A. Loria, P.J. Nicklasson and H. Sira-Ramirez, *Passivity-based control of Euler-Lagrange systems*, Springer-Verlag, Berlin, Communications and Control Engineering, 3rd ed., 2014.
13. R. Ortega. L.P. Borja. J. Romero and A. Donaire, *PID Passivity-based Control of Nonlinear Systems with Applications*, J. Wiley and Sons, 2021.
14. H. Rodriguez, R. Ortega, G. Escobar and N. Barabanov: A robustly stable output feedback saturated controller for the boost dc-to-dc converter, *Systems and Control Letters*, Vol. 40, No. 1, pp. 1 -8, May 2000.
15. A.H.R. Rosa,, L.M.F. Morais, G.O. Fortes and S.I. Seleme Jr, Practical considerations of nonlinear control techniques applied to static power converters: A survey and comparative study, *Electrical Power and Energy Systems*, vol. 127, 106545, 2021.
16. S. R. Sanders and G. C. Verghese Lyapunov-based control for switched power converters, *IEEE Trans. Power Electronics*, vol. 7. no 1, pp. 17-24, 1992
17. H. Sira, R. Perez, R. Ortega and M. Garcia, Passivity-based controllers for the stabilization of DC-to-DC power converters, *Automatica*, Vol. 39, No. 4, pp. 499-513, May, 1997.
18. A. van der Schaft, *L₂-Gain and Passivity Techniques in Nonlinear Control*, Springer, Berlin, 3rd Edition, 2016.

19. M. Zhang, R. Ortega, Z. Liu and H. Su: A new family of interconnection and damping assignment passivity-based controllers, *Int. J. on Robust and Nonlinear Control*, Vol. 27, No. 1, pp. 50-65, 2017.

□

APPENDIX

A MAPLE COMPUTATION OF THE TERM $a_1 a_2 - a_0$

$$\begin{aligned} > \#r := \frac{\sqrt{-4d1 d2 ys^2 + 1}}{2}; \\ > a2 := \frac{Kp}{2 \cdot d1} + \frac{Kp \cdot r}{d1} + d1 + d2; a1 := \text{simplify}\left(\frac{(\frac{1}{2} - r - u0 ys)^2}{ys^2} + \left(-\frac{Kp(\frac{1}{2} - r - u0 ys)}{Ki} + \frac{2u0(\frac{1}{2} - r - u0 ys)}{ys Ki} + \frac{\frac{1}{2} + r}{d1}\right)Ki + \left(\frac{1}{2} + r - u0 ys\right)Kp + d1 d2 + u0^2\right); a0 := 2 \cdot Ki \cdot r; \end{aligned}$$

$$a2 := \frac{Kp}{2d1} + \frac{Kpr}{d1} + d1 + d2$$

$$a1 := \frac{4d1^2 d2 ys^2 + (8rKp ys^2 + 4(r - \frac{1}{2})^2)d1 + 4Ki(\frac{1}{2} + r)ys^2}{4ys^2 d1}$$

$$a0 := 2Ki r$$

$$> f1 := \text{simplify}(8 \cdot ys^2 \cdot d1^2 \cdot (a1 \cdot a2 - a0));$$

$$\begin{aligned} f1 := & 8d1^4 d2 ys^2 + (16Kpr ys^2 + 8d2^2 ys^2 + 8r^2 - 8r + 2) d1^3 \\ & + (8r^2 d2 + ((24Kpd2 - 8Ki) ys^2 - 8d2) r \\ & + (4Kpd2 + 4Ki) ys^2 + 2d2) d1^2 \\ & + (8r^3 Kp + (16Kp^2 ys^2 - 4Kp)r^2 \\ & + ((8Kpd2 + 8Kp^2) ys^2 - 2Kp)r + 4Kid2 ys^2 + Kp) d1 \\ & + 8ys^2 Ki \left(\frac{1}{2} + r\right)^2 Kp \end{aligned}$$

$$p1(r) := d1^3(8r^2 - 8r + 2)$$

$$p2(r) := d2d1^3(8r^2 - 8r + 2) + d1^2(-8Kiy s^2 r + 4Kiy s^2)$$

$$p3(r) := 8Kpd1r(r^2 - \frac{r}{2} - \frac{1}{4})$$